

1 Estimating forest aboveground biomass with terrestrial laser scanning: 2 current status and future directions

3 Running title: Estimating forest AGB with TLS

4 **Miro Demol**^{1,2,*}, **Hans Verbeeck**¹, **Bert Gielen**², **John Armston**³, **Andrew Burt**⁴, **Mathias Disney**^{4,5},
5 **Laura Duncanson**³, **Jan Hackenberg**⁶, **Daniel Kükenbrink**⁷, **Alvaro Lau**⁸, **Pierre Ploton**⁹, **Artie Sew-**
6 **dien**¹⁰, **Atticus Stovall**^{3,11}, **Stéphane Momo Takoudjou**^{9,12}, **Liubov Volkova**¹³, **Chris Weston**¹³, **Virginia**
7 **Wortel**¹⁰ and **Kim Calders**¹

8 ¹CAVElab, Computational and Applied Vegetation Ecology, Department of Environment, Faculty of Bioscience Engi-
9 neering, Ghent University, Ghent, Belgium

10 ²PLECO, Plants and Ecosystems, Faculty of Science, Antwerp University, Wilrijk, Belgium

11 ³Department of Geographical Sciences, University of Maryland, College Park, MD 20742, USA

12 ⁴Department of Geography, University College London, London, UK

13 ⁵NERC NCEO-UCL

14 ⁶Independent developer of free software - Aachener Str. 5d, 56072 Koblenz, Germany

15 ⁷Swiss Federal Institute WSL, Zürichstrasse 111, CH-8903 Birmensdorf, Switzerland

16 ⁸Wageningen University, Laboratory of Geo-Information Science and Remote Sensing, Droevendaalsesteeg 3, 6708 PB
17 Wageningen, the Netherlands

18 ⁹AMAP, Univ Montpellier, IRD, CNRS, INRAE, CIRAD, Montpellier, France

19 ¹⁰Department of Forest Management, Centre for Agricultural Research in Suriname (CELOS), Prof.Dr.Ir.J.Ruinardlaan 1,
20 Paramaribo, Suriname

21 ¹¹NASA Goddard Space Flight Center, 8800 Greenbelt Rd., Greenbelt, MD, United States

22 ¹²Plant Systematic and Ecology Laboratory (LaBosystE), Department of Biology, Higher Teachers' Training College,
23 University of Yaoundé I, P.O. Box 047, Yaoundé, Cameroon

24 ¹³School of Ecosystem and Forest Sciences, The University of Melbourne, Victoria 3010, Australia

5 * Corresponding Author: Miro Demol; Coupure Links 653, 9000, Ghent, Belgium, mirodemol@hotmail.com

Abstract

1 Improving the global monitoring of aboveground biomass (AGB) is crucial for forest management to be effective in climate mitigation. In the last decade, methods have been developed for estimating AGB from terrestrial laser scanning (TLS) data. TLS-derived AGB estimates can address current uncertainties in allometric and Earth observation (EO) methods that quantify AGB.

2 We assembled a global dataset of TLS scanned and consecutively destructively measured trees from a variety of forest conditions and reconstruction pipelines. The dataset comprised 391 trees from 111 species with stem diameter ranging 8.5 to 180.3 cm and AGB ranging 13.5 – 43,950 kg.

3 TLS-derived AGB closely agreed with destructive values (bias < 1%, concordance correlation coefficient of 98%). However, we identified below-average performances for smaller trees (< 1,000 kg) and conifers. In every individual study, TLS estimates of AGB were less biased and more accurate than those from allometric scaling models (ASMs), especially for larger trees (> 1,000 kg).

4 More effort should go to further understanding and constraining several TLS error sources. We currently lack an objective method of evaluating point cloud quality for tree volume reconstruction, hindering the development of reconstruction algorithms and presenting a bottleneck for tracking down the error sources identified in our synthesis. Since quantifying AGB with TLS requires only a fraction of the efforts as compared to destructive harvesting, TLS-calibrated ASMs can become a powerful tool in AGB upscaling. TLS will be critical for calibrating/validating scheduled and launched remote sensing initiatives aiming at global AGB mapping.

Keywords:

Aboveground biomass, terrestrial laser scanning, carbon, Quantitative Structure Modelling, 3D reconstruction, allometric scaling models, REDD+

1 A decade of terrestrial laser scanning for forest aboveground biomass estimation

Forests can help mitigate climate change (by sequestering carbon through forest growth and subsequent storage in the soil), but loss of forest carbon (e.g. from deforestation) can also accelerate climate change. Improved land-use and forest management aimed at curbing forest loss (e.g. through mechanisms such as Reducing Emissions from Deforestation and forest Degradation (REDD+)) require accurate data sources to enable monitoring of forest carbon stocks at a global scale. Remote sensing enables systematic forest mapping and monitoring, focusing on quantifying woody aboveground biomass (AGB). To estimate AGB from satellite data, field estimates are required, which are conventionally generated

55 through measurements of diameter at breast height (DBH) and, if possible, tree height (TH), wood density, and tree species
56 information are collected in the field. These measurements are then converted to AGB using allometric scaling models
57 (ASMs).

58 New developments in earth observation (EO) demand a substantial increase in the accuracy and precision of field
59 reference AGB. This is particularly important given a suite of new and forthcoming EO missions, such as NASA's GEDI
60 (Dubayah *et al.*, 2020), NASA-ISRO SAR (NISAR) (Rosen *et al.*, 2015), ICESat-2 (Narine *et al.*, 2019) and the forthcoming
61 ESA BIOMASS (Quegan *et al.*, 2019) missions. While these will all collect data sensitive to 3D forest structure and biomass,
62 they do not directly measure AGB, and thus rely heavily on field data. The calibration and validation of EO mission biomass
63 products requires field AGB which is currently only available through ASM estimates (Duncanson *et al.*, 2019, 2021). Yet,
64 ASMs can be problematic for a number of reasons (Duncanson *et al.*, 2017), mostly pertaining to the model selection
65 uncertainties (Picard *et al.*, 2015), the general lack of traceability and assumptions of metabolic scaling that may or may
66 not be valid (Zhou *et al.*, 2021). In addition, the current method to obtain reference AGB for ASM calibration involves
67 destructively harvesting trees. This is expensive, invasive and not always ethically or legally possible. Consequently, ASMs
68 always have to rely on limited calibration data with questionable spatial and tree size representativity.

69 In recent years, a number of studies have demonstrated that terrestrial laser scanning (TLS) can be an alternative,
70 more accurate and precise approach to estimate AGB at tree and stand scale. TLS allows rapid capture of a highly detailed
71 3D point cloud of the forest environment (Calders *et al.*, 2020). Several algorithms have been developed that enclose the
72 tree point cloud to create a volume reconstruction that can be converted to an estimate of AGB using wood basic density
73 (ρ_{basic} ; ratio of oven-dry mass and green volume). These algorithms can be classified into two types: (1) voxel techniques
74 that partition the tree point cloud in cubes or so-called voxels and estimate volume based on the fraction of filled voxels
75 (Bienert *et al.*, 2014); and (2) Quantitative Structure Modelling (QSM) methods that aim at reconstructing the full woody
76 volume of trees by fitting geometrical primitives through the tree point cloud (Hackenberg *et al.*, 2014; Raumonon *et al.*,
7 2013). Some methods employ a hybrid method of both voxel filling and geometric fitting (Stovall *et al.*, 2017).

78 **2 TLS-derived AGB validation experiments: a synthesis**

79 Destructive measurements of AGB are useful for developing ASMs but can also be used for benchmarking TLS-based
80 AGB methods. Here, we pooled and re-analysed the results of ten TLS-derived biomass studies that were validated
81 using destructive tree harvesting and, together, cover all forested continents (Table 1 and Fig. 1). This joint destructive
82 dataset features 391 trees from 111 species (20 undetermined trees) with DBH ranging 8.5 to 180.3 cm, corresponding
83 to a reference AGB range of 14 kg – 43,950 kg. TLS scans were acquired with five different scanner types. Two QSM
84 methods (TreeQSM (Raumonon *et al.*, 2013) and SimpleForest (Hackenberg *et al.*, 2015)) and one hybrid voxelisation
85 method (outer hull modelling (Stovall *et al.*, 2017)) were used to obtain volume estimates. All studies were conducted
86 in forest environments, except Kükenbrink *et al.* (2021) who sampled urban trees. All studies applied a tree-centered
87 scanning approach sensu Wilkes *et al.* (2017), except for the data collected in Demol *et al.* (2021b) who applied a grid-wise
88 procedure. All foliage conditions were represented, that is, coniferous needle-on/off, and broadleaf leaf-on/off. Point cloud

89 post-processing differed between studies. Most notably, there was diversity in the coregistration algorithms, the filtering
90 procedures, whether or not leaves were stripped from the point clouds and which leaf stripping methods were used, and
91 the downsampling procedures. Finally, tree volume from TLS was converted to AGB using basic wood density.

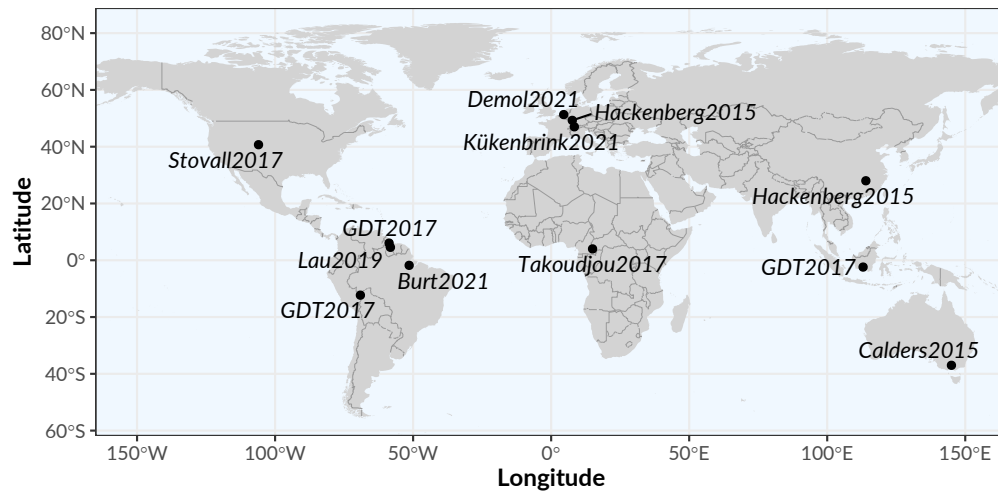


Figure 1: Site location of the destructive harvesting experiments included in the meta-analysis. Data from Hackenberg *et al.* (2015); Calders *et al.* (2015); Stovall *et al.* (2017); Lau *et al.* (2019); Kükenbrink *et al.* (2021); Demol *et al.* (2021a); Momo Takoudjou *et al.* (2018); Burt *et al.* (2021). GDT = Gonzalez de Tanago *et al.* (2018).

92 Reference AGB was obtained either by direct weighing, by measuring the outer diameters and length of tree segments,
93 or by a combination of the two. Dry matter content (DMC; the ratio of the dry mass and fresh mass of a wood sample) was
94 used to convert fresh weightings to AGB. The formula of Smalian (Goulding, 1979) was used to infer tree volume from
95 diameter/length measurements, which was converted to AGB with ρ_{basic} . The specificity of the wood properties varied from
96 being sourced from databases (Gonzalez de Tanago *et al.*, 2018; Stovall *et al.*, 2017) over DBH- and species-dependent
97 local models (Demol *et al.*, 2021a; Calders *et al.*, 2015) to volume- and mass-weighted per-tree values (Burt *et al.*, 2021).
98 AGB was also predicted with species- or genus-specific, or pantropical ASMs, using DBH and if available tree height as
99 predictors (Table 2). If required in the model, we used the same value for ρ as in the original study. We calculated bias (b)
100 as the sum of the residual AGB divided by the sum of the harvested AGB. Additionally, we tested if harvested (reference)
101 AGB and ASM/TLS-derived AGB corresponded with the 1:1 line by computing the significance of the coefficients of a linear
102 regression of the form: $AGB_{\text{ASM}} - AGB_{\text{harvest}} = \alpha + \beta * AGB_{\text{ASM}}$ and $AGB_{\text{TLS}} - AGB_{\text{harvest}} = \alpha + \beta * AGB_{\text{TLS}}$ (Valbuena *et al.*,
103 2017; Piñeiro *et al.*, 2008). Models correspond to the 1:1 line if the null hypotheses $H_0 : \alpha = 0$ and $H_0 : \beta = 1$ are not
104 rejected.

105 3 Results from the synthesis

106 Across these 10 studies, TLS-derived AGB was in accordance with destructive values (Fig. 2). The total destructively
107 assessed AGB was 1,174 Mg versus a nearly unbiased TLS estimate of 1,183 Mg (b of +0.75% and the RMSE of 1140 kg).

108 The concordance correlation coefficient (CCC) between destructive and TLS AGB was 98.3%. For the individual studies *b*
 109 ranged from -9.5% to +22%. For every study, the CCC was > 96%, except for the data from Demol *et al.* (2021b) (CCC of
 110 85%) and Lau *et al.* (unpublished) (CCC of 88%).

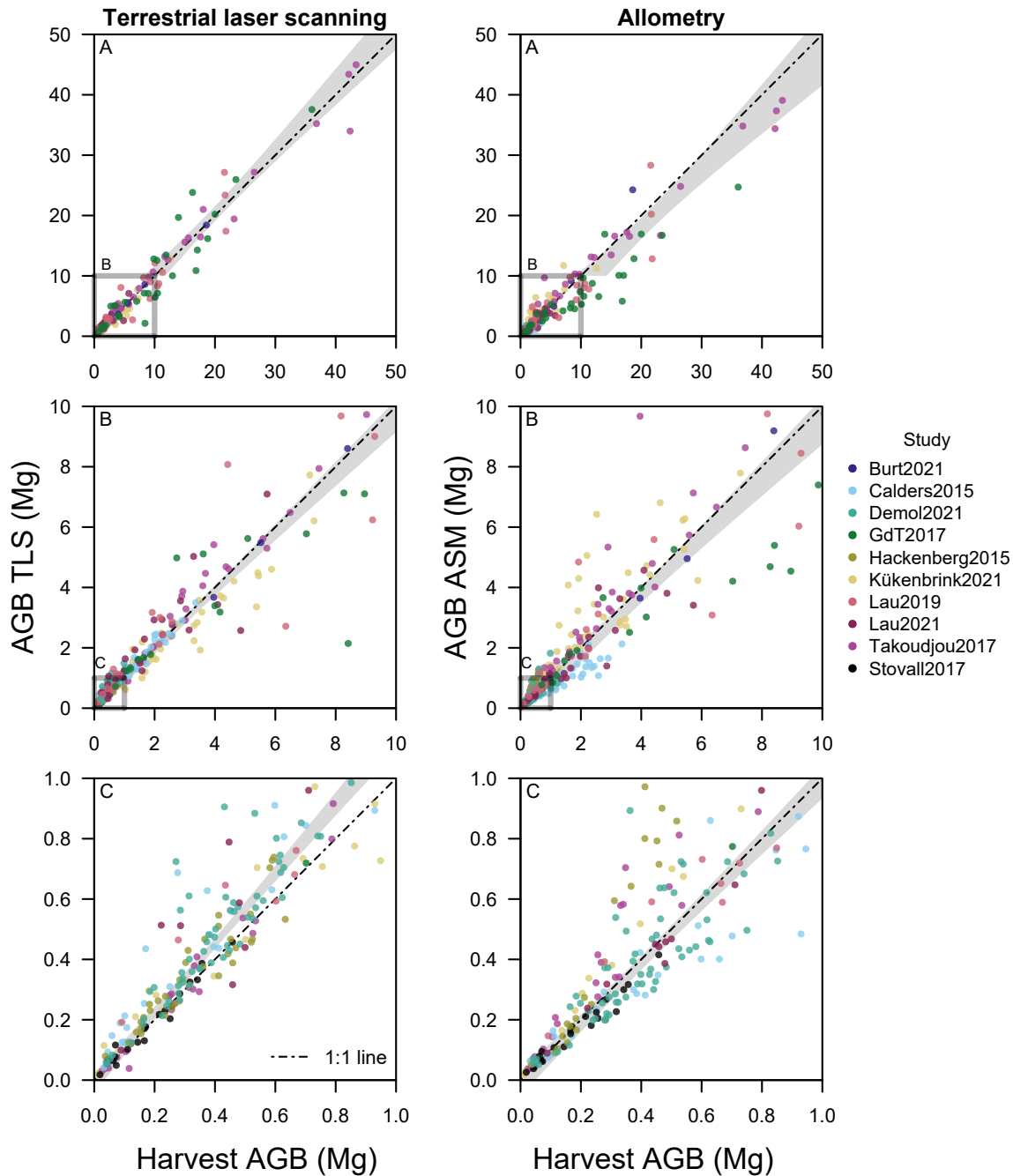


Figure 2: Comparison of destructively assessed aboveground biomass (AGB) and estimates from terrestrial laser scanning (left) and allometric scaling models (right). Each point represents one tree. Points are coloured by study (see Table 1 for a method overview of each study). For visualisation purposes the axes are truncated in B (up to 10 Mg) and C (up to 1 Mg). The 95% confidence interval of a linear regression of the form $AGB_{\text{harvest}} = a + b * AGB_{\text{TLS/ASM}}$ truncated to the same limits is added in grey.

111 The TLS method performed less well for conifers ($n = 69$, $b = +16\%$, $CCC = 88\%$) than for broadleaves ($n = 322$, $b =$
 112 $+0.47\%$, $CCC = 98.2\%$). Conifers in the dataset were in general much smaller than broadleaf trees (mean AGB of 312
 113 kg and 3,600 kg, respectively). Trees that were foliated during data acquisition were slightly overestimated ($n = 281$, $b =$
 114 $+1.4\%$, $CCC = 98.2\%$), whereas leafless and needleless trees were underestimated ($n = 110$, $b = -3.8\%$, $CCC = 97.4\%$).
 115 The TLS-derived AGB of trees lighter than 1,000 kg AGB was overestimated ($n = 216$, $b = 19.7\%$, $CCC = 87\%$). This
 116 phenomenon occurred for all small trees regardless of site and study and contrasts with the nearly unbiased estimates
 117 for trees $> 1,000$ kg AGB ($n = 176$, $b = 0.62\%$, $CCC = 98\%$). Biomass of trees of intermediate size (between 1,000 and
 118 10,000 kg) was also fairly well estimated with TLS ($n = 142$, $b = 0.34\%$, $CCC = 90\%$). This results was confirmed with the
 119 hypothesis tests (Table 3), with a significant ($p < 0.001$) β coefficient for TLS-derived AGB for trees lighter than 1,000 kg.
 120 TLS-derived tropical tree biomass was nearly unbiased ($n = 148$, $b = +0.69\%$, $CCC = 97.9\%$), while temperate tree AGB
 121 was slightly underestimated ($n = 178$, $b = -2.60\%$, $CCC = 97.7\%$). The only sub-tropical study (Calders *et al.*, 2015) had an
 122 AGB overestimation of 9.7% ($n = 65$, Table 1).

123 ASMs sourced from literature performed less well in predicting AGB than TLS. For every individual study, ASM-predicted
 124 AGB was less precise and less accurate and had a lower CCC than its TLS-derived counterpart (Table 1 and 2). Overall,
 125 ASM-derived AGB was underestimated by 7.8% (whereas 0.75% for TLS), the RMSE was 1,730 kg (whereas 1140 kg for
 126 TLS) and the CCC was lowered to 95.6% (whereas 98.3% for TLS). Residual AGB increased with DBH for both TLS and
 127 ASM estimates (Fig. 3) albeit increasing stronger for the latter.

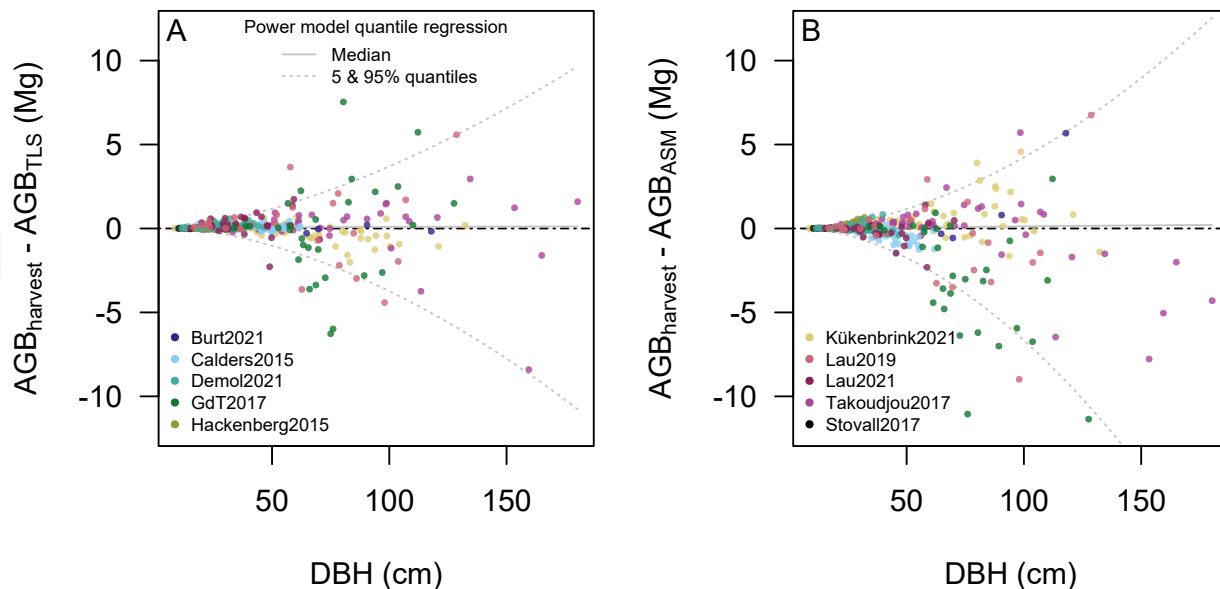


Figure 3: Residual tree aboveground biomass (AGB) against diameter at breast (DBH). Residual AGB was calculated as the estimated AGB minus the reference AGB from harvesting. Panel A contains the TLS-derived AGB estimates and panel B contains the allometric estimates. The grey lines represent the median (solid) and 5% and 95% quantiles (dotted) of a power model quantile regression. The black dash-dotted line indicates residuals are zero. Contributing study legend is split in two panels.

4 Insights from the synthesis

Here we show that TLS is already successfully applied for estimating AGB over a large range of forest types and TLS methods. This synthesis showcases new insights and increased experience with TLS over the years. For instance, the scanning grid size in Calders *et al.* (2015) of 40 meters would, today, be regarded as sparse for volumetric reconstructions, especially for forests that are more dense and complex. Results from Momo Takoudjou *et al.* (2018) have been truncated to 5 cm diameter and needed manual interaction to correct erroneous cylinder fits, while applying a different QSM method (TreeQSM or SimpleForest instead of SimpleTree) might have allowed fully automatic full volume extraction. The adverse effects of wind on the scan image quality are currently better understood; for reference measurements, windy scan acquisition conditions as in Hackenberg *et al.* (2015) should have been avoided. Using the new generation of faster scanners will allow reducing wind effects in scan images by scanning in between windy periods. Leaf-on reconstructions (such as in Calders *et al.* (2015); Demol *et al.* (2021b)) could be improved by applying a suitable leaf-stripping algorithm. The oldest included TLS data was collected in 2012. It is likely that using present-day knowledge and methods would further increase concordance, as the knowledge base of TLS in forestry has rapidly expanded in recent years (Calders *et al.*, 2020).

Nevertheless, several sources of error need to be further constrained. For correctly segmented point cloud data, we identify four causes of inaccurate volume estimations: 1) misalignment in the scan data due to wind and coregistration inaccuracies; 2) foliage interference; 3) scattering errors when the beam footprint is partially intersecting; and 4) occlusion and sparse point cloud issues. AGB of smaller trees was generally overestimated with TLS. This suggests they share a common, more fundamental cause of volume overestimation (that is, if wood basic density conversion errors are not considered, and if we assume tree reconstruction algorithms to be scale-invariant). Quantitative evidence that only very recently emerged showed that small branches are disproportionately impacted by misalignment and scattering errors (Vaaja *et al.*, 2016; Abegg *et al.*, 2021; Wilkes *et al.*, 2021) and that these errors tended to overestimate rather than to underestimate branch dimensions (Hackenberg *et al.*, 2015). Smaller trees have proportionally more small branches and foliage, which introduces another level of uncertainty in TLS reconstructions.

New developments in coregistration, scattering filters (Wilkes *et al.*, 2021) and foliage separation algorithms (Vicari *et al.*, 2019; Wang and Fang, 2020; Krishna Moorthy *et al.*, 2020) are projected to mitigate these errors. Occlusion is most effectively avoided with improving data acquisition protocols (Wilkes *et al.*, 2017) yet can be to some extent overcome with QSMs. Therefore, while we advise to be well aware of the aforementioned error sources when modelling volumes of small trees or branches, we do not expect these to stand in the way of future tree volume estimates using TLS.

Destructive approaches for obtaining reference biomass values also have several caveats. First, direct weighings are preferred over sectioned measurements of tree dimensions (converted to volume using Smalian, Huber) (Goulding, 1979). Second, converting fresh mass (or green volume for sectional measurements) to AGB needs precise quantification of wood properties such as dry matter content or green density (Hackenberg *et al.*, 2015; Sagang *et al.*, 2018; Demol *et al.*, 2021a; Burt *et al.*, 2021). Last, material lost during these operations (branch loss when felling the tree, chainsaw swarf) can be substantial (Burt *et al.*, 2021). These considerations are important for future validation studies.

5 Perspective: Towards a point cloud quality index

Our synthesis showcased the thriving diversity in forest point cloud datasets and processing pipelines. These methods have drastically improved (see Synthesis). The most recent studies, Burt *et al.* (2021) and Kükenbrink *et al.* (2021), have implemented these best-practices and achieved comparatively best results in respectively evergreen trees and leaf-off trees. Our synthesis included older studies that, retrospectively, applied suboptimal methods. We argue that our pooled dataset can be regarded as representative for an operational, real-life implementation of TLS for AGB quantification. It is encouraging that TLS-derived AGB estimates in this synthesis were in good agreement with harvested values and were nearly unbiased.

It is highly unlikely that a single scanner, or tree segmentation procedure, or leaf-stripping algorithm, or volume reconstruction method, performs best in all circumstances. Therefore, we think data collection and processing pipeline diversity should be encouraged and further strengthened. Currently state-of-the-art scanners are prohibitively expensive for certain groups and some software is proprietary or requires thorough IT knowledge, requiring more democratization and automation before large-scale TLS can be implemented (Disney *et al.*, 2018). Segmenting single trees from forest point clouds is currently one of the most time-consuming steps in the pipeline, especially for complex tropical forests (Martin-Ducup *et al.*, 2021). Automatic tree segmentation algorithms (Burt *et al.*, 2018; Wang *et al.*, 2020) allow drastically increasing the number of tree AGB observations with TLS - something that would represent colossal efforts if to be achieved by destructive measurements (Stovall *et al.*, 2017).

Operational TLS campaigns will no longer be accompanied by destructive validation experiments. How trustworthy are point clouds from future TLS missions for tree volume reconstruction? Currently, there is no objective way of assessing point cloud quality across different datasets in the context of 3D tree modelling, yet this is indispensable for the intercomparability of TLS data (Calders *et al.*, 2020). Meticulously recording metadata is a must (but unfortunately not consistently done): providing a detailed description of TLS data acquisition (scanner type and settings, scan position layout and meteorological conditions) and post-processing procedures (coregistration, filtering, downsampling, tree segmentation) is indispensable. Conversely, applying identical procedures in different forest types (or different seasons; cf. foliage condition) is no guarantee for similar point cloud quality.

Alternatively, indices that objectively grade point cloud quality could be calculated for single tree point clouds a posteriori as a proxy for the accuracy of TLS-derived estimates. To our knowledge, no such index currently exists. This hinders the development of reconstruction algorithms (as testing data is not intercomparable) and can be a bottleneck for tracking down the error sources outlined in our synthesis. Such indexes could be quite simple (e.g. point density variation in the tree point cloud, point count normalised by tree size) or more complex (e.g. occlusion mapping approaches in voxel space or ray tracing simulations (Schneider *et al.*, 2019)).

A benchmarking dataset is a powerful tool to develop such a point cloud quality index and could at the same time provide testing data for reconstruction modellers. For this, the data from the experiments that were synthesised here could serve, supplemented by new simultaneous TLS and reference measurements of tree mass from harvesting (Clark and Kellner, 2012), as well as measurements at finer scales such as individual branch dimensions. To improve geographical

198 and climatic coverage, more data is needed from boreal and sub-tropical biomes (Fig. 1).

199 **6 An outlook on implementing TLS for global biomass mapping**

200 TLS-based tree inventories have become popular because they are versatile and enable fast measurements of novel
201 structural data. Within this synthesis exercise, we showed that TLS is not only a capable alternative to allometric models,
202 but also performed better across a global set of forest AGB observations. This is an encouraging and timely finding
203 given the importance of accurate reference data for EO product calibration and validation, and improved land-use and
204 forest management toward climate change mitigation (Duncanson *et al.*, 2021). This is particularly important for trees
205 where destructive harvesting is unavailable or logistically impractical (e.g. in previously understudied forest types or where
206 conventional allometries are poorly calibrated). TLS seems to be particularly well suited for the characterisation of big trees
207 that also contain most carbon (Bastin *et al.*, 2018; Disney *et al.*, 2020). Where destructive measurements are undesirable
208 or impossible (urban and heritage trees, protected or remote areas,...) TLS is the only (tested) alternative to ASMs (Stovall
209 *et al.*, 2017; Lau *et al.*, 2019).

210 TLS campaigns for estimating the volume of individual trees (e.g. for calibration of allometric equations) are not
211 necessarily comparable to plot-scale campaigns (e.g. for upscaling and remote sensing calibration objectives). All except
212 one of the included studies used a tree-centered scanning approach. Tree-centered scanning likely results in reduced
213 occlusion compared to a grid-wise approach, especially for dense environments with multiple canopy layers and leaf-on
214 conditions. One obvious disadvantage is that TLS is not able to provide information on the inside of the tree: internal decay
215 or cavities cannot be mapped (but whether or not this is represented in harvest data underpinning ASMs is also unclear).

216 Whereas we conclude that TLS has the potential to provide higher accuracy AGB estimates than traditional ASM
217 approaches, TLS data are currently far less available than traditional tree measurements. Methodological and practical
218 advances propel the increased collection and availability of TLS, yet significant funding and logistical support would be
219 required to operationally replace existing field estimates with TLS. At present, TLS represents an important pathway forward
220 to complement and improve traditional estimates. Floristic inventories remain important to complement TLS missions, as
221 well as wood basic density measurements (da Páscoa *et al.*, 2020; Momo *et al.*, 2020; Demol *et al.*, 2021a).

222 Overall, the nature of the current limitations in TLS (small trees, foliage,...) is not fundamental but technical. We expect
223 significantly improved TLS-estimates of AGB by applying the best current and imminent methods. In our opinion, TLS
224 will therefore be crucial for the calibration of several remote sensing biomass products (possibly through intermediary
225 sensors, e.g. UAV or airborne laser scanning) (Stovall *et al.*, 2018; Duncanson *et al.*, 2021). Specifically, the development
226 of non-destructive ASMs with TLS will enable the widespread application of high-quality tree-level biomass predictions to
227 existing global forest inventory plots. Fundamental questions of tree scaling, inter alia the ASM assumption of invariant tree
228 mass scaling with size, remain open. Potential uncertainty and bias in ASM-predicted AGB, particularly for large trees, can
229 be assessed using destructive harvesting and TLS. Robustly validated remote sensing biomass products will be critical to
230 the effectiveness of carbon financing markets, while strengthening REDD+ type of initiatives by bringing more objective
231 AGB estimates to the table.

232 **Acknowledgements**

233 Collecting reference tree biomass data is hard work. We sincerely thank the many, many people involved in the field and
234 lab work that made this study possible.

235 **Conflict of Interest Statement**

236 The authors declare that the research was conducted in the absence of any commercial or financial relationships that
237 could be construed as a potential conflict of interest.

238 **Author Contributions**

239 Miro Demol: methodology; formal analysis; investigation; writing—original draft. Kim Calders, Hans Verbeeck, Bert Gielen:
240 conceptualisation; resources; funding acquisitions. Miro Demol, Andy Burt, Jan Hackenberg, Daniel Kükenbrink, Alvaro
241 Lau, Pierre Ploton, Artie Sewdien, Atticus Stovall, Momo Takoudjou, Liubov Volkova, Chris Weston, Virginia Wortel, Kim
242 Calders: data collection and processing. All Authors: writing (review and editing).

243 **Funding**

244 MD was funded by the European Union's Horizon 2020 research and innovation programme under grant agreement
245 no 730944—RINGO: Readiness of ICOS for Necessities of Integrated Global Observations. The Research Foundation
246 Flanders (FWO) supported ICOS Flanders and ICOS ETC. KC was funded by the European Union's Horizon 2020
247 research and innovation programme under the Marie Skłodowska-Curie grant agreement No 835398. DK was supported
248 by the Swiss National Forest Inventory. MDY acknowledges funding from Natural Environment Research Council grant
249 NE/N00373X/1, ERC grant no. 757526, and capital and travel funding from NERC NCEO and UCL.

250 **Supplemental Data**

251 There is no Supplementary Material document associated with this manuscript.

252 **Data Availability Statement**

253 The dataset generated and analysed for this study can be found in a Zenodo repository: doi.org/10.5281/zenodo.5236762.

References

- Abegg M, Boesch R, Schaepman M. E, and Morsdorf F. Impact of Beam Diameter and Scanning Approach on Point Cloud Quality of Terrestrial Laser Scanning in Forests. *IEEE Transactions on Geoscience and Remote Sensing*, 59(10): 8153–8167, oct 2021. doi: 10.1109/TGRS.2020.3037763.
- Bastin J, Rutishauser E, Kellner J. R, Saatchi S, Pélissier R, Hérault B, Slik F, Bogaert J, De Cannière C, Marshall A. R, Poulsen J, Alvarez-Loyaza P, Andrade A, Angbonga-Basia A, Araujo-Murakami A, Arroyo L, Ayyappan N, de Azevedo C. P, Banki O, Barbier N, Barroso J. G, Beeckman H, Bitariho R, Boeckx P, Boehning-Gaese K, Brandão H, Brearley F. Q, Breuer Ndoundou Hockemba M, Brienen R, Camargo J. L. C, Campos-Arceiz A, Cassart B, Chave J, Chazdon R, Chuyong G, Clark D. B, Clark C. J, Condit R, Honorio Coronado E. N, Davidar P, de Haulleville T, Descroix L, Doucet J, Dourdain A, Droissart V, Duncan T, Silva Espejo J, Espinosa S, Farwig N, Fayolle A, Feldpausch T. R, Ferraz A, Fletcher C, Gajapersad K, Gillet J, do Amaral I. L, Gonmadje C, Grogan J, Harris D, Herzog S. K, Homeier J, Hubau W, Hubbell S. P, Hufkens K, Hurtado J, Kamdem N. G, Kearsley E, Kenfack D, Kessler M, Labrière N, Laumonier Y, Laurance S, Laurance W. F, Lewis S. L, Libalah M. B, Ligot G, Lloyd J, Lovejoy T. E, Malhi Y, Marimon B. S, Marimon Junior B. H, Martin E. H, Matius P, Meyer V, Mendoza Bautista C, Monteagudo-Mendoza A, Mtui A, Neill D, Parada Gutierrez G. A, Pardo G, Parren M, Parthasarathy N, Phillips O. L, Pitman N. C. A, Ploton P, Ponette Q, Ramesh B. R, Razafimahaimodison J, Réjou-Méchain M, Rolim S. G, Saltos H. R, Rossi L. M. B, Spironello W. R, Rovero F, Saner P, Sasaki D, Schulze M, Silveira M, Singh J, Sist P, Sonke B, Soto J. D, de Souza C. R, Stropp J, Sullivan M. J. P, Swanepoel B, ter Steege H, Terborgh J, Texier N, Toma T, Valencia R, Valenzuela L, Ferreira L. V, Valverde F. C, Van Andel T. R, Vasque R, Verbeeck H, Vivek P, Vleminckx J, Vos V. A, Wagner F. H, Warsudi P. P, Wortel V, Zagt R. J, and Zebaze D. Pan-tropical prediction of forest structure from the largest trees. *Global Ecology and Biogeography*, 27(11): 1366–1383, nov 2018. doi: 10.1111/geb.12803.
- Bienert A, Hess C, Maas H.-G, and von Oheimb G. A voxel-based technique to estimate the volume of trees from terrestrial laser scanner data. *The International Archives of the Photogrammetry, Remote Sensing and Spatial Information Sciences*, XL-5(5):101–106, jun 2014. doi: 10.5194/isprsarchives-XL-5-101-2014.
- Burt A, Disney M, and Calders K. Extracting individual trees from lidar point clouds using treeSeg. *Methods in Ecology and Evolution*, 10(3):2041–210X.13121, dec 2018. doi: 10.1111/2041-210X.13121.
- Burt A, Boni Vicari M, da Costa A. C. L, Coughlin I, Meir P, Rowland L, and Disney M. New insights into large tropical tree mass and structure from direct harvest and terrestrial lidar. *Royal Society Open Science*, 8(2):rsos.201458, feb 2021. doi: 10.1098/rsos.201458.
- Calders K, Newnham G, Burt A, Murphy S, Raumonon P, Herold M, Culvenor D, Avitabile V, Disney M, Armston J, and Kaasalainen M. Nondestructive estimates of above-ground biomass using terrestrial laser scanning. *Methods in Ecology and Evolution*, 6(2):198–208, feb 2015. doi: 10.1111/2041-210X.12301.
- Calders K, Adams J, Armston J, Bartholomeus H, Bauwens S, Bentley L. P, Chave J, Danson F. M, Demol M, Disney M,

- 287 Gaulton R, Krishna Moorthy S. M, Levick S. R, Saarinen N, Schaaf C, Stovall A, Terry L, Wilkes P, and Verbeeck H.
288 Terrestrial laser scanning in forest ecology: Expanding the horizon. *Remote Sensing of Environment*, 251:112102, dec
289 2020. doi: 10.1016/j.rse.2020.112102.
- 290 Chave J, Coomes D, Jansen S, Lewis S. L, Swenson N. G, and Zanne A. E. Towards a worldwide wood economics
291 spectrum. *Ecology Letters*, 12(4):351–366, apr 2009. doi: 10.1111/j.1461-0248.2009.01285.x.
- 292 Chave J, Réjou-Méchain M, Búrquez A, Chidumayo E, Colgan M. S, Delitti W. B, Duque A, Eid T, Fearnside P. M,
293 Goodman R. C, Henry M, Martínez-Yrizar A, Mugasha W. A, Muller-Landau H. C, Mencuccini M, Nelson B. W,
294 Ngomanda A, Nogueira E. M, Ortiz-Malavassi E, Pélissier R, Ploton P, Ryan C. M, Saldarriaga J. G, and Vieilledent G.
295 Improved allometric models to estimate the aboveground biomass of tropical trees. *Global Change Biology*, 20(10):
296 3177–3190, 2014. doi: 10.1111/gcb.12629.
- 297 Chojnacky D. C, Heath L. S, and Jenkins J. C. Updated generalized biomass equations for North American tree species.
298 *Forestry*, 87(1):129–151, 2014. doi: 10.1093/forestry/cpt053.
- 299 Clark D. B and Kellner J. R. Tropical forest biomass estimation and the fallacy of misplaced concreteness. *Journal of*
300 *Vegetation Science*, 23(6):1191–1196, dec 2012. doi: 10.1111/j.1654-1103.2012.01471.x.
- 301 da Páscoa K. J. V, Gomide L. R, Tng D. Y. P, Scolforo J. R. S, Filho A. C. F, and de Mello J. M. How many trees and samples
302 are adequate for estimating wood-specific gravity across different tropical forests? *Trees - Structure and Function*, 34(6):
303 1383–1395, 2020. doi: 10.1007/s00468-020-02007-5.
- 304 Demol M, Calders K, Krishna Moorthy S. M, Van den Bulcke J, Verbeeck H, and Gielen B. Consequences of vertical basic
305 wood density variation on the estimation of aboveground biomass with terrestrial laser scanning. *Trees*, 35(2):671–684,
306 apr 2021a. doi: 10.1007/s00468-020-02067-7.
- 307 Demol M, Calders K, Verbeeck H, and Gielen B. Forest above-ground volume assessments with terrestrial laser scanning:
308 a ground-truth validation experiment in temperate, managed forests. *Annals of Botany*, 128(6):805–819, oct 2021b. doi:
309 10.1093/aob/mcab110.
- 310 Disney M. I, Boni Vicari M, Burt A, Calders K, Lewis S. L, Raunonen P, and Wilkes P. Weighing trees with lasers: advances,
311 challenges and opportunities. *Interface Focus*, 8(2):20170048, apr 2018. doi: 10.1098/rsfs.2017.0048.
- 312 Disney M, Burt A, Wilkes P, Armston J, and Duncanson L. New 3D measurements of large redwood trees for biomass and
313 structure. *Scientific Reports*, 10(1):16721, dec 2020. doi: 10.1038/s41598-020-73733-6.
- 314 Dubayah R, Blair J. B, Goetz S, Fatoyinbo L, Hansen M, Healey S, Hofton M, Hurtt G, Kellner J, Luthcke S, Armston J,
315 Tang H, Duncanson L, Hancock S, Jantz P, Marselis S, Patterson P. L, Qi W, and Silva C. The Global Ecosystem
316 Dynamics Investigation: High-resolution laser ranging of the Earth's forests and topography. *Science of Remote Sensing*,
317 1:100002, jun 2020. doi: 10.1016/j.srs.2020.100002.

- 318 Duncanson L, Armston J, Disney M, Avitabile V, Barbier N, Calders K, Carter S, Chave J, Herold M, Crowther T. W,
319 Falkowski M, Kellner J. R, Labrière N, Lucas R, MacBean N, McRoberts R. E, Meyer V, Næsset E, Nickeson J. E,
320 Paul K. I, Phillips O. L, Réjou-Méchain M, Román M, Roxburgh S, Saatchi S, Schepaschenko D, Scipal K, Siqueira P. R,
321 Whitehurst A, and Williams M. The Importance of Consistent Global Forest Aboveground Biomass Product Validation.
322 *Surveys in Geophysics*, 40(4):979–999, jul 2019. doi: 10.1007/s10712-019-09538-8.
- 323 Duncanson L, Huang W, Johnson K, Swatantran A, McRoberts R. E, and Dubayah R. Implications of allometric model
324 selection for county-level biomass mapping. *Carbon Balance and Management*, 12(1), oct 2017. doi: 10.1186/
325 s13021-017-0086-9.
- 326 Duncanson L, Armston J, Disney M, Avitabile V, Barbier N, Calders K, Carter S, Chave J, Herold M, MacBean N,
327 McRoberts R, Minor D, Paul K, Réjou-Méchain M, Roxburgh S, Williams M, Albinet C, Baker T, Bartholomeus H,
328 Bastin J, Coomes D, Crowther T, Davies S, de Bruin S, De Kauwe M, Domke G, Dubayah R, Falkowski M, Fatoyinbo L,
329 Goetz S, Jantz P, Jonckheere I, Jucker T, Kay H, Kellner J, Labriere N, Lucas R, Mitchard E, Morsdorf F, Naeset E,
330 Park T, Phillips O, Ploton P, Quegan S, Saatchi S, Schaaf C, Schepaschenko D, Scipal K, Stovall A, Thiel C, Wulder M,
331 Camacho F, Nickeson J, Román M, and Margolis H. Aboveground Woody Biomass Product Validation Good Practices
332 Protocol. Version 1.0. *Good Practices for Satellite Derived Land Product Validation*, page 236, 2021. doi: 10.5067/doc/
333 ceoswgcv/lpv/agb.001.
- 334 Forrester D. I, Tachauer I. H, Annighoefer P, Barbeito I, Pretzsch H, Ruiz-Peinado R, Stark H, Vacchiano G, Zlatanov T,
335 Chakraborty T, Saha S, and Sileshi G. W. Generalized biomass and leaf area allometric equations for European tree
336 species incorporating stand structure, tree age and climate. *Forest Ecology and Management*, 396:160–175, jul 2017.
337 doi: 10.1016/j.foreco.2017.04.011.
- 338 Gonzalez de Tanago J, Lau A, Bartholomeus H, Herold M, Avitabile V, Raunonen P, Martius C, Goodman R. C, Disney M,
339 Manuri S, Burt A, and Calders K. Estimation of above-ground biomass of large tropical trees with terrestrial LiDAR.
340 *Methods in Ecology and Evolution*, 9(2):223–234, feb 2018. doi: 10.1111/2041-210X.12904.
- 341 Goulding C. J. Cubic spline curves and calculation of volume of sectionally measured trees. *New Zealand Journal of*
342 *Forestry Science*, 9(1):89–99, 1979.
- 343 Hackenberg J, Morhart C, Sheppard J, Spiecker H, and Disney M. Highly accurate tree models derived from terrestrial
344 laser scan data: A method description. *Forests*, 5(5):1069–1105, 2014. doi: 10.3390/f5051069.
- 345 Hackenberg J, Spiecker H, Calders K, Disney M, and Raunonen P. SimpleTree - An efficient open source tool to build tree
346 models from TLS clouds. *Forests*, 6(11):4245–4294, 2015. doi: 10.3390/f6114245.
- 347 Herold M, Carter S, Avitabile V, Espejo A. B, Jonckheere I, Lucas R, McRoberts R. E, Næsset E, Nightingale J, Petersen R,
348 Reiche J, Romijn E, Rosenqvist A, Rozendaal D. M, Seifert F. M, Sanz M. J, and De Sy V. The Role and Need for
349 Space-Based Forest Biomass-Related Measurements in Environmental Management and Policy. *Surveys in Geophysics*,
350 40(4):757–778, 2019. doi: 10.1007/s10712-019-09510-6.

- 351 Krishna Moorthy S. M, Raunonen P, Van den Bulcke J, Calders K, and Verbeeck H. Terrestrial laser scanning for
352 non-destructive estimates of liana stem biomass. *Forest Ecology and Management*, 456(August 2019):117751, 2020.
353 doi: 10.1016/j.foreco.2019.117751.
- 354 Kükenbrink D, Gardi O, Morsdorf F, Thürig E, Schellenberger A, and Mathys L. Above-ground biomass references for
355 urban trees from terrestrial laser scanning data. *Annals of Botany*, pages 1–16, 2021. doi: 10.1093/aob/mcab002.
- 356 Lau A, Martius C, Bartholomeus H, Shenkin A, Jackson T, Malhi Y, Herold M, and Bentley L. P. Estimating architecture-
357 based metabolic scaling exponents of tropical trees using terrestrial LiDAR and 3D modelling. *Forest Ecology and*
358 *Management*, 439(March):132–145, 2019. doi: 10.1016/j.foreco.2019.02.019.
- 359 Lin L. I.-k. A Concordance Correlation Coefficient to Evaluate Reproducibility. *Biometrics*, 45(1):255, mar 1989. doi:
360 10.2307/2532051.
- 361 Martin-Ducup O, Mofack G, Wang D, Raunonen P, Ploton P, Sonké B, Barbier N, Coueron P, and Pélissier R. Evaluation
362 of automated pipelines for tree and plot metric estimation from TLS data in tropical forest areas. *Annals of Botany*, 128
363 (6):753–766, 2021. doi: 10.1093/aob/mcab051.
- 364 Momo S. T, Ploton P, Martin-Ducup O, Lehnebach R, Fortunel C, Sagang L. B. T, Boyemba F, Coueron P, Fayolle A,
365 Libalah M, Loumeto J, Medjibe V, Ngomanda A, Obiang D, Pélissier R, Rossi V, Yongo O, Bocko Y, Fonton N, Kamdem N,
366 Katembo J, Kondaoule H. J, Maïdou H. M, Mankou G, Mbası M, Mengui T, Mofack G. I, Moundounga C, Moundounga Q,
367 Nguimbous L, Ncham N. N, Asue F. O. M, Senguela Y. P, Viard L, Zapfack L, Sonké B, and Barbier N. Leveraging
368 Signatures of Plant Functional Strategies in Wood Density Profiles of African Trees to Correct Mass Estimations From
369 Terrestrial Laser Data. *Scientific Reports*, 10(1):1–11, 2020. doi: 10.1038/s41598-020-58733-w.
- 370 Momo Takoudjou S, Ploton P, Sonké B, Hackenberg J, Griffon S, de Coligny F, Kamdem N. G, Libalah M, Mofack G, Le
371 Moguédec G, Pélissier R, and Barbier N. Using terrestrial laser scanning data to estimate large tropical trees biomass
372 and calibrate allometric models: A comparison with traditional destructive approach. *Methods in Ecology and Evolution*,
373 9(4):905–916, 2018. doi: 10.1111/2041-210X.12933.
- 374 Narine L. L, Popescu S, Neuenschwander A, Zhou T, Srinivasan S, and Harbeck K. Estimating aboveground biomass and
375 forest canopy cover with simulated ICESat-2 data. *Remote Sensing of Environment*, 224(January):1–11, 2019. doi:
376 10.1016/j.rse.2019.01.037.
- 377 Paul K. I, Roxburgh S. H, England J. R, Ritson P, Hobbs T, Brooksbank K, John Raison R, Larmour J. S, Murphy S,
378 Norris J, Neumann C, Lewis T, Jonson J, Carter J. L, McArthur G, Barton C, and Rose B. Development and testing of
379 allometric equations for estimating above-ground biomass of mixed-species environmental plantings. *Forest Ecology*
380 *and Management*, 310:483–494, 2013. doi: 10.1016/j.foreco.2013.08.054.
- 381 Picard N, Rutishauser E, Ploton P, Ngomanda A, and Henry M. Should tree biomass allometry be restricted to power
382 models? *Forest Ecology and Management*, 353:156–163, 2015. doi: 10.1016/j.foreco.2015.05.035.

- 383 Piñeiro G, Perelman S, Guerschman J. P, and Paruelo J. M. How to evaluate models: Observed vs. predicted or predicted
384 vs. observed? *Ecological Modelling*, 216(3-4):316–322, sep 2008. doi: 10.1016/j.ecolmodel.2008.05.006.
- 385 Quegan S, Le Toan T, Chave J, Dall J, Exbrayat J. F, Minh D. H. T, Lomas M, D’Alessandro M. M, Paillou P, Papathanassiou K,
386 Rocca F, Saatchi S, Scipal K, Shugart H, Smallman T. L, Soja M. J, Tebaldini S, Ulander L, Villard L, and Williams M.
387 The European Space Agency BIOMASS mission: Measuring forest above-ground biomass from space. *Remote Sensing*
388 *of Environment*, 227(March 2019):44–60, 2019. doi: 10.1016/j.rse.2019.03.032.
- 389 Raumonon P, Kaasalainen M, Åkerblom M, Kaasalainen S, Kaartinen H, Vastaranta M, Holopainen M, Disney M, and
390 Lewis P. Fast Automatic Precision Tree Models from Terrestrial Laser Scanner Data. *Remote Sensing*, 5(2):491–520,
391 jan 2013. doi: 10.3390/rs5020491.
- 392 Rosen P. A, Hensley S, Shaffer S, Veilleux L, Chakraborty M, Misra T, Bhan R, Raju Sagi V, and Satish R. The NASA-ISRO
393 SAR mission - An international space partnership for science and societal benefit. *IEEE National Radar Conference -*
394 *Proceedings*, 2015-June(June):1610–1613, 2015. doi: 10.1109/RADAR.2015.7131255.
- 395 Sagang L. B. T, Momo S. T, Libalah M. B, Rossi V, Fonton N, Mofack G. I, Kamdem N. G, Nguetsop V. F, Sonké B, Ploton P,
396 and Barbier N. Using volume-weighted average wood specific gravity of trees reduces bias in aboveground biomass
397 predictions from forest volume data. *Forest Ecology and Management*, 424(November 2017):519–528, 2018. doi:
398 10.1016/j.foreco.2018.04.054.
- 399 Schneider F. D, Kükenbrink D, Schaepman M. E, Schimel D. S, and Morsdorf F. Quantifying 3D structure and occlusion in
400 dense tropical and temperate forests using close-range LiDAR. *Agricultural and Forest Meteorology*, 268(November
401 2018):249–257, 2019. doi: 10.1016/j.agrformet.2019.01.033.
- 402 Stovall A. E, Vorster A. G, Anderson R. S, Evangelista P. H, and Shugart H. H. Non-destructive aboveground biomass
estimation of coniferous trees using terrestrial LiDAR. *Remote Sensing of Environment*, 200(August):31–42, 2017. doi:
404 10.1016/j.rse.2017.08.013.
- 405 Stovall A. E, Shugart H. H, Stovall A. E, Anderson-Teixeira K. J, and Anderson-Teixeira K. J. Assessing terrestrial laser
406 scanning for developing non-destructive biomass allometry. *Forest Ecology and Management*, 427(May):217–229, 2018.
407 doi: 10.1016/j.foreco.2018.06.004.
- 408 Vaaja M. T, Virtanen J.-P, Kurkela M, Lehtola V, Hyyppä J, and Hyyppä H. the Effect of Wind on Tree Stem Parameter
409 Estimation Using Terrestrial Laser Scanning. *ISPRS Annals of Photogrammetry, Remote Sensing and Spatial Information*
410 *Sciences*, III-8(July):117–122, 2016. doi: 10.5194/isprsannals-iii-8-117-2016.
- 411 Valbuena R, Hernando A, Manzanera J, Görgens E, Almeida D, Mauro F, García-Abril A, and Coomes D. Enhancing of
412 accuracy assessment for forest above-ground biomass estimates obtained from remote sensing via hypothesis testing
413 and overfitting evaluation. *Ecological Modelling*, 366:15–26, dec 2017. doi: 10.1016/j.ecolmodel.2017.10.009.

- 414 Vicari M. B, Disney M, Wilkes P, Burt A, Calders K, and Woodgate W. Leaf and wood classification framework for terrestrial
415 LiDAR point clouds. *Methods in Ecology and Evolution*, 10(5):680–694, 2019. doi: 10.1111/2041-210X.13144.
- 416 Wang D, Momo Takoudjou S, and Casella E. LeWoS: A universal leaf-wood classification method to facilitate the 3D
417 modelling of large tropical trees using terrestrial LiDAR. *Methods in Ecology and Evolution*, 11(3):376–389, mar 2020.
418 doi: 10.1111/2041-210X.13342.
- 419 Wang Y and Fang H. Estimation of LAI with the LiDAR technology: A review. *Remote Sensing*, 12(20):1–28, 2020. doi:
420 10.3390/rs12203457.
- 421 Wilkes P, Lau A, Disney M, Calders K, Burt A, Gonzalez de Tanago J, Bartholomeus H, Brede B, and Herold M. Data
422 acquisition considerations for Terrestrial Laser Scanning of forest plots. *Remote Sensing of Environment*, 196:140–153,
23 2017. doi: 10.1016/j.rse.2017.04.030.
- 424 Wilkes P, Shenkin A, Disney M, Malhi Y, Bentley L. P, and Vicari M. B. Terrestrial laser scanning to reconstruct branch
425 architecture from harvested branches. *Methods in Ecology and Evolution*, 2021(August):1–14, 2021. doi: 10.1111/
426 2041-210X.13709.
- 427 Xiang W, Liu S, Deng X, Shen A, Lei X, Tian D, Zhao M, and Peng C. General allometric equations and biomass allocation
428 of *Pinus massoniana* trees on a regional scale in southern China. *Ecological Research*, 26(4):697–711, 2011. doi:
429 10.1007/s11284-011-0829-0.
- 430 Zhou X, Yang M, Liu Z, Li P, Xie B, and Peng C. Dynamic allometric scaling of tree biomass and size. *Nature Plants*, 7(1):
431 42–49, 2021. doi: 10.1038/s41477-020-00815-8.

Table 1: [continued on next page.] Overview of the destructive reference datasets, including data acquisition settings and conditions, processing pipelines to remove foliage, reconstruct tree volume, number of scanned and harvested trees (n), tree species, diameter at breast height (DBH), summary of destructive harvest methodology and wood basic density sampling. Prediction performance indicators for aboveground biomass (AGB) estimates with terrestrial laser scanning (TLS) and allometric scaling models (ASMs) are provided as bias, root mean square error (RMSE) and concordance correlation coefficient (CCC, Lin (1989)).

Reference	Country	Scanner	Foliage	Leaf stripping	Reconstruction method	Scan pattern	Wind? ^a	n
Burt <i>et al.</i> (2021)	Brazil	RIEGL VZ-400	leaf-on	TLSeparation v1.2.1.5	TreeQSM 2.3.2	8 around	NA	4
Calders <i>et al.</i> (2015)	Australia	RIEGL VZ-400	leaf-on	No	TreeQSM 2.0	Cross + centre, 5 pos total. 40m sides	NA	65
Demol <i>et al.</i> (2021b)	Belgium	RIEGL VZ-400; VZ-1000	leaf-off; needle-on; needle-off	No	TreeQSM 2.30	Grid (s = 20 m)	No	65
Gonzalez de Tanago <i>et al.</i> (2018)	Peru Guyana Indonesia	RIEGL VZ-400	leaf-on	No	TreeQSM 2.0	8 or 13 scans/tree	No	29
Hackenberg <i>et al.</i> (2015)	Germany China	Z+F IMAGER 5010	leaf-off; leaf-on; needle-on	Yes No No	SimpleForest	6-8 around	Yes Yes	36
Küktenbrink <i>et al.</i> (2021)	China Switz.	RIEGL VZ-1000	leaf-off ^b	Manual, few trees	TreeQSM 2.3.1	3-4 pos per tree	Yes	55
Lau <i>et al.</i> (2019)	Guyana	RIEGL VZ-400	leaf-on	TLSeparation	TreeQSM 2.0	8-10 around	NA	26
Lau <i>et al.</i> (unpublished)	Suriname	RIEGL VZ-400	leaf-on	LeWoS	TreeQSM 2.3.3	8-10 around	NA	28
Momo Takoudjou <i>et al.</i> (2018)	Cameroon	Leica C10	leaf-on	Manual	SimpleTree, manual corrections	Multiple scans around single trees	NA	61
Stovall <i>et al.</i> (2017)	USA	FARO Focus 120	needle-on, needle-off	Voxel-based	Outer Hull Modelling + voxelisation	3-4 pos per tree	No	22
OVERALL	12 countries	5 scanner models	4 foliage conditions		3 method families			391

GWDD = global wood density database (Chave *et al.*, 2009); **NA** = not applicable; **DMC** = dry matter content; **TLSeparation** = see Vicari *et al.* (2019); **Lewos** = see Wang and Fang (2020); **BH** = breast height = 130 cm; **DBH** = diameter at BH, **WD** = wood basic density.

^a The results from Hackenberg *et al.* (2015) were reprocessed with SimpleForest (instead of SimpleTree) using reverse pipe model.

^a No: no wind or precipitation; Yes: wind or precipitation; NA: wind and precipitation conditions unknown.

^b Except for three conifers.

[Continued from previous page.]

Reference	Species	DBH mean (min- max) cm	Destructive validation method	AGB TLS Bias (%) RMSE (kg) CCC	AGB ASM Bias (%) RMSE (kg) CCC	ASM Type ^c
Burt <i>et al.</i> (2021)	4 different	86 (65-118)	On-site weighing of full tree. Conversion to AGB with mass-weighted DMC from wood discs sampled in different tree compartments.	-0.81 98 1	15.3 2885 .92	Pt
Calders <i>et al.</i> (2015)	<i>Eucalyptus leucoxylon</i> <i>E. microcarpa</i> <i>E. tricarpa</i> <i>Pinus sylvestris</i>	35 (11-62)	On-site weighing of full tree. Discs at BH or every 3 m along stem for subset of trees; DBH-dependent DMC relation.	9.7 171 .98	-29.8 491 .78	Sp
Demol <i>et al.</i> (2021b)	<i>Fagus sylvatica</i> <i>Larix decidua</i> <i>Fraxinus excelsior</i>	29 (11-47)	On-site weighing of full tree. DMC from discs at BH (and every 3 m after BH for subset of trees). Volume-weighted DMC correction.	22.4 165 .85	2.7 201 .76	Sp
Gonzalez de Tanago <i>et al.</i> (2018)	several species	73 (34-128)	Diameter measurements every meter until taper of 10 cm; Smalian. Branches with d _i 10 cm disregarded.	-1.6 2949 0.94	-29.4 4495 .81	Pt
Hackenberg <i>et al.</i> (2015)	<i>Quercus petraea</i> <i>Erythrophloeum fordii</i> <i>Pinus massoniana</i>	24 (13-32)	On-site weighing of tree in compartments. Discs at multiple heights along the stem; mass-weighted DMC (excluding bark).	68 .92 -9.5	315 .58 21.7	Sp
Kükenbrink <i>et al.</i> (2021)	29 different	59 (9-132)	Weighing of full tree. Discs at different diameter compartments in the tree for DMC.	556 .97 1.7	1197 .89 -7.8	Sp
Lau <i>et al.</i> (2019)	several species	58 (17-129)	Fresh mass measured directly on field. Smalian for stems and large branches. GWDD for WD conversions.	2038 0.96 12.7	2676 .92 -10.1	Pt
Lau <i>et al.</i> (unpublished)	several species	38 (15-70)	Diameter measurements every meter until taper of 10 cm; Smalian. Branches with d _i 10 cm disregarded.	728 0.88 0.6	658 .88 -1.7	Pt
Momo Takoudjou <i>et al.</i> (2018)	15 different species	59 (11-180)	Combination of weighing and Smalian. Volume-weighted conversion to AGB with DMC and green density.	1355 0.99 -0.5	1853 0.98 -10.1	Pt
Stovall <i>et al.</i> (2017)	<i>Pinus contorta</i>	21 (10-34)	Weighing of full tree. DMC from stem discs and branch samples. WD from species-specific literature.	20 .99	33 0.96	Gn
OVERALL	111 tree species; 20 unknown	45 (8.5-180)		0.75% 1141 kg .98	-7.79% 1728 kg .956	

^c Pt = Pantropical; Sp = species-specific; Gn = genus-specific

Table 2: Allometric scaling models to derive aboveground biomass (AGB) from predictor variable diameter at breast height (DBH, from field inventory) with additionally tree height (h) and wood basic density (ρ). In Kükenbrink *et al.* (2021) AGB is modelled from the stem volume V_{stem} and volume expansion factor (VEF). Wood basic density was either obtained from literature (ρ_{GWDD} , from Chave *et al.* (2009)), or by sampling wood disc specimens in the destructive measurements and computing a volume-weighted (ρ_{vw}) or mass-weighted (ρ_{mw}) average. Whenever possible, a species-specific model was used with field-measured DBH as predictor variable. Tree height, on the contrary, was taken from reference measurements on the felled tree (as tree height measurements from ground observations were often incomplete).

Dataset	Model form	Type	Source
Burt <i>et al.</i> (2021)	$AGB = .067(DBH^2 \cdot h \cdot \rho_{mw})^{.976}$	Pantropical	Chave <i>et al.</i> (2014)
Calders <i>et al.</i> (2015)	$AGB = a \cdot DBH^b$	Species-specific	Paul <i>et al.</i> (2013)
Demol <i>et al.</i> (2021b)	$AGB = a \cdot DBH^b$	Species-specific	Forrester <i>et al.</i> (2017)
Hackenberg <i>et al.</i> (2015)	$AGB = a \cdot DBH^b$	Species-specific	Xiang <i>et al.</i> (2011); Forrester <i>et al.</i> (2017)
Gonzalez de Tanago <i>et al.</i> (2018); Lau <i>et al.</i> (2019)	$AGB = .067(DBH^2 \cdot h \cdot \rho_{\text{GWDD}})^{.976}$	Pantropical	Chave <i>et al.</i> (2014)
Momo Takoudjou <i>et al.</i> (2018)	$AGB = .067(DBH^2 \cdot h \cdot \rho_{vw})^{.976}$	Pantropical	Chave <i>et al.</i> (2014)
Kükenbrink <i>et al.</i> (2021)	$AGB = V_{\text{stem}} \cdot \rho_{vw} \cdot VEF^{(*)}$	Species-specific	Swiss NFI; Herold <i>et al.</i> (2019)
Stovall <i>et al.</i> (2017)	$AGB = a \cdot DBH^b$	Genus-specific	Chojnacky <i>et al.</i> (2014)

* Stem volume in Kükenbrink *et al.* (2021) is modelled with a combination of tree and site characteristics: $V_{\text{stem}} = f(\text{DBH, site index, elevation, dominant diameter, canopy layer, bifurcation})$.

Table 3: Coefficients and standard errors (*se*) of a linear regression between the harvested AGB (AGB_{harvest}) and either AGB from terrestrial laser scanning (TLS) or allometric scaling models (ASM) ($AGB_{\text{TLS/ASM}}$ respectively): $AGB_{\text{harvest}} = a + b * AGB_{\text{TLS/ASM}}$. Significances of the associated hypothesis tests sensu Piñeiro *et al.* (2008); Valbuena *et al.* (2017) to test for agreement with the 1:1 line (Fig. 2) taking the form $AGB_{\text{TLS/ASM}} - AGB_{\text{harvest}} = \alpha + \beta * AGB_{\text{TLS/ASM}}$ (in Mg) are added (only one model disagreed significantly with the 1:1 line; ***: $p < 0.001$).

	TLS		ASM	
	<i>a</i> (Mg, \pm se)	<i>b</i> (\pm se)	<i>a</i> (Mg, \pm se)	<i>b</i> (\pm se)
AGB > 10 Mg	0.312 (\pm 1.386)	0.97 (\pm 0.06)	1.108 (\pm 2.140)	1.05 (\pm 0.10)
1 Mg < AGB < 10 Mg	-0.061 (\pm 0.146)	1.04 (\pm 0.04)	0.018 (\pm 0.257)	1.06 (\pm 0.06)
AGB < 1 Mg	0.006 (\pm 0.014)	0.87 (\pm 0.03) ***	0.008 (\pm 0.021)	1.01 (\pm 0.04)